



Hard Cr₂O₃ coatings on SS316L substrates prepared by reactive magnetron sputtering technique: a potential candidate for orthopedic implants

Masoud Mohammadtaheri¹ · Yuanshi Li¹ · Qiaoqin Yang¹

Received: 22 October 2018 / Accepted: 26 March 2019 / Published online: 17 April 2019
© Springer-Verlag GmbH Germany, part of Springer Nature 2019

Abstract

316L stainless steel (SS) implants suffer from tribological and biocompatibility problems which limit their service lifetime. In order to improve the surface properties of 316L SS for orthopedic implant applications, hard chromium oxide coatings were applied on 316L SS substrates using a reactive magnetron sputtering technique. The morphological, structural, and phase compositional analyses were conducted on the deposited coatings by scanning electron microscopy, X-ray diffraction, Raman spectroscopy, and X-ray photoelectron spectroscopy. The Rockwell-C indentation tests were performed on the coated substrates to qualitatively evaluate the adhesion of coatings on the steel substrates. The surface characteristics of coatings were measured by using an optical profilometer. The mechanical properties of coatings were reported by measuring the Hardness and Young's modulus. The corrosion resistance of coated and uncoated SS substrates was compared using potentiodynamic polarization tests. An inductively coupled plasma optical emission spectrometry (ICP-OES) was employed to analyze the biocompatibility of the samples by measuring the amount of toxic Cr ions released after the immersion test. The results show that the coatings are adherent and composed of a single Cr₂O₃ phase with a hardness of 25 to 29 GPa. The corrosion resistance of the SS has been improved by applying a chromium oxide coating. The coated SS samples have also demonstrated better wear resistance and lower friction coefficient compared to bare SS samples under a reciprocating sliding condition in saline solution. The biocompatibility of the SS has been enhanced by the Cr₂O₃ coating as much less Cr ions were released after immersion tests. These results indicate that the hard Cr₂O₃ coatings can be considered as a candidate for extending the lifetime of SS implants.

Keywords Chromium oxide · Coatings · Orthopedic implants · Reactive magnetron sputtering · SS316L · Wear resistance · Corrosion

Introduction

316L SS has been widely used for orthopedic implants due to the comprehensive characters of low cost, high toughness, high corrosion resistance, and superior mechanical properties. However, 316L steel possesses a low hardness and it readily suffers from early degradation under wear and corrosion interactions (Ningshen et al. 2006; Liu et al. 2009). Therefore, hard non-toxic corrosion resistant coatings which also adhere very

well to substrates are required to solve the tribo-corrosion problems for orthopedic implant applications. This is due to the fact that tribological and corrosion processes substantially influence the biocompatibility of materials. For instance, pains, pseudotumor formation, and inflammation in patients are the direct effects of wear debris and toxic ions released by Fe, Cr, and Ni chemical element presented in 316L SS which, however, can be prevented by applying a wear, corrosion, and biocompatible protective coating material on the implant surface (Oje and Ogwu 2017). In this context, various ceramic coatings have been employed by different researchers for biomedical applications. Among them, diamond-like carbon (DLC), chromium nitride (CrN), hydroxyapatite (HA), titanium nitride (TiN), and titanium niobium nitride (TiNbN) have been extensively investigated (Fisher et al. 2002, 2004; Roy and Lee 2007; Serro et al. 2009; Love et al. 2013; Gotman and Gutmanas 2014; van Hove et al. 2015; Oje and Ogwu 2017). TiN and TiNbN coatings have

Responsible editor: Philippe Garrigues

✉ Qiaoqin Yang
qiaoqin.yang@usask.ca

¹ Department of Mechanical Engineering, University of Saskatchewan, 57 Campus Drive, Saskatoon, SK S7H 5A9, Canada

been commercially used in hip and knee prostheses, while other coating systems are still under the different stages of investigation (Serro et al. 2009; Gotman and Gutmanas 2014; Oje and Ogwu 2017). DLC coatings show poor adhesion on the substrates due to a high level of internal stress generated during the coating process, and a severe delamination of DLC coatings usually occurs during *in vivo* tests which is still the main drawback for practical application (Anttila et al. 1999; Taeger et al. 2003). HA coatings, due to their poor toughness and high brittleness, are not desired in applications where the material is subjected to various loading regimes, despite their excellent bi-material properties (Charalambous 2014; Oje and Ogwu 2017). The present authors in their recent research (Mohammadtaheri et al. 2018) showed that Cr_2O_3 coatings can reach a hardness value of up to 29.5 GPa which was in agreement with the hardness value mentioned for bulk Cr_2O_3 in earlier literature (Samsonov 1973; Kainarskii and Degtyareva 1977; Kao et al. 1989; Hones et al. 1999). Cr_2O_3 also possesses interesting properties such as low coefficient of friction, high wear, and corrosion resistance, which making it potential protective coatings for many applications (Bhushan et al. 1997; Ji et al. 2004; Pang et al. 2008). To obtain Cr_2O_3 coatings, different techniques such as plasma-spray (Singh et al. 2012; Dong et al. 2013; Babu et al. 2018), sputtering (Contoux et al. 1997; Luo et al. 2008), chemical vapor deposition (CVD) (Carta et al. 2005), pulsed laser deposition (Monnereau et al. 2010), and laser-assisted chemical vapor deposition (Sousa et al. 2011) have already been used. However, high-quality Cr_2O_3 coatings with hardness as high as bulk Cr_2O_3 have only obtained by sputtering techniques so far (Hones et al. 1999; Luo et al. 2007, 2008; Lin and Sproul 2015; Mohammadtaheri et al. 2018). Metallic chromium, due to its different valance state, can form various chromium oxide compounds, including CrO_3 , Cr_8O_{21} , Cr_5O_{12} , $\text{CrO}_{2.906}$, CrO_2 , Cr_3O_4 , Cr_2O_3 , CrO , and Cr_3O (Kainarskii and Degtyareva 1977; Barshilia and Rajam 2008; Lin and Sproul 2015). It has been confirmed that depending on the preparation method and deposition conditions, chromium oxides with different oxidation states, microstructure, chemical composition, and mechanical properties can be formed. For instance, in RF-magnetron sputtering coating process, single-phase Cr_2O_3 coatings with a hardness value of over 25 GPa can only be produced in a specific deposition condition (i.e., at room temperature, at a low pressure of 1.6×10^{-1} Pa, where Cr-target voltage and oxygen content are 260 V and between 15 and 25 vol% of total gas, respectively (Mohammadtaheri et al. 2018)). Cr_2O_3 coatings have already been used for various applications, such as advanced heat engines (LACKEY et al. 1987), digital magnetic recording units (Bhushan et al. 1997), gas bearing applications (Bhushan 1981), electronics (Sourty et al. 2003), and optics (Trube 1993; Liu et al. 2009). However, to the best of authors' knowledge, comprehensive investigations on the application of chromium oxide coatings for biomedical implants have not been performed yet. We have recently established a correlation

between phase composition, microstructure, and mechanical properties of chromium oxide coatings and the deposition parameters in a reactive magnetron sputtering technique (Mohammadtaheri et al. 2018). Now, in this research, authors are determined to continue the previous research and conduct a detailed study on the potential application of such hard chromium oxide coatings for biomedical applications. In the current research, tribological properties, corrosion, adhesion, and biocompatibility behavior of reactively sputtered chromium oxide coatings prepared on 316L SS are tested according to the international standards when they are exposed to the physiological saline solution.

Materials and methods

A RF-magnetron coater (SPLD620-FLR made by Plasmionique Inc., Rimouski, QC, Canada) was used to deposit chromium coatings on mirror-polished AISI 316L SS substrates with the dimension of $25 \text{ mm} \times 25 \text{ mm} \times 5 \text{ mm}$. A 76.2 mm-diameter Cr-target plate (99.95% pure) was installed in the system to produce chromium oxide coatings in the simultaneous presence of argon and oxygen plasma. The deposition parameters (Table 1) were the optimum ones determined from our previous research (Mohammadtaheri et al. 2018) in which chromium oxide coatings with a hardness value as high as bulk Cr_2O_3 ($H \sim 29$ GPa) have been produced.

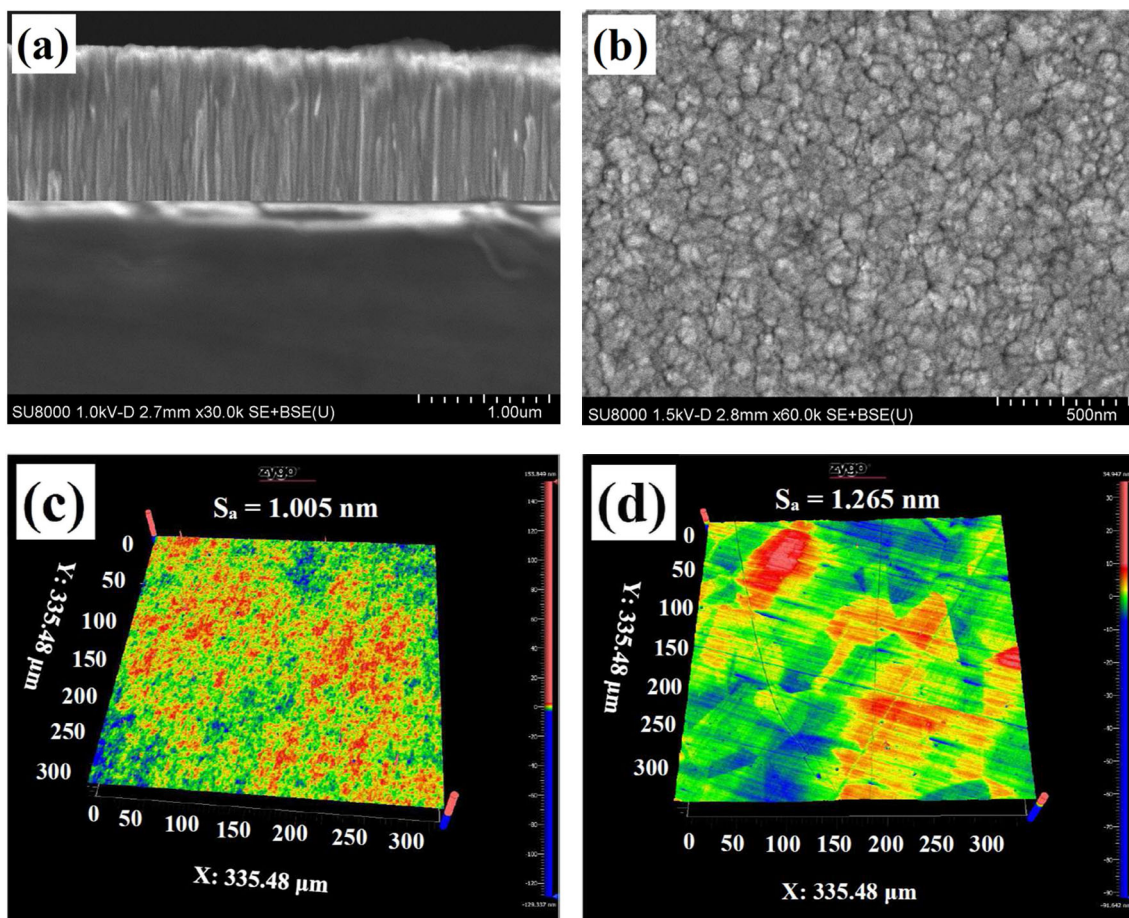
The mean roughness (R_a) and wear volume of coatings were measured with the aid of an optical profilometer (New View 8000, manufactured by Zygo Corporation, Middlefield, CT, USA). The system was equipped with a $\times 50$ Mirau objective and using a standard filter type (bandwidth 125 nm for the light with $\lambda = 550$ nm) for surface characterization measurements. Grazing incidence XRD (Rigaku XRD Ultima IV, $\text{CuK}\alpha$ radiation) technique at incidence angle of $\theta = 7^\circ$ was used to investigate the phase composition of the coatings. X'Pert HighScore Plus software was employed to compare the obtained XRD patterns with the standard databases (known as PDF files) to identify the chromium oxide peaks. Raman spectroscopy (Renishaw 2000 spectroscope, argon laser source $\lambda = 514$ nm, $P = 0.5$ mW) was used to identify different oxide states and support the XRD patterns. A silicon reference sample was used to calibrate the Raman spectroscope and the peak positions were fitted with the aid of Wire.3.3 software. The oxidation state of metallic chromium in the coatings was determined by X-ray photoelectron spectroscopy (XPS). The spectrometer used in this method was a Kratos Axis Ultra model with a monochromatic Al $\text{K}\alpha$ radiation made by Kratos Analytical Ltd., Manchester, UK. Before XPS measurements, the surface contaminants were removed by sputtering the surface of coatings with Ar ions for 20 s. To compensate the charge effects during XPS analysis of insulating oxide coatings, the high-resolution spectrum of adventitious hydrocarbon was also

Table 1 Deposition parameters for the hard Cr₂O₃ coating

Cr-target power (W)	Cr-target voltage (V)	Ar flow rate (sccm)	O ₂ flow rate (sccm)	Temperature (°C)	Pressure (Pa)
360	260	30	5	150	0.16

monitored. The morphological characteristics of the coatings were observed by a scanning electron microscope (SEM). To evaluate the adhesion properties of coatings qualitatively, Rockwell “C” Indentation with a load of 981 N (100 kgf) was performed on three different areas of coatings according to ISO 26443 standard (ISO 26443 2002). The imprints were then observed subsequently using an optical microscope. The hardness and Young’s modulus of coatings were measured by nanoindentation technique (UMT with a Berkovich indenter at 3 mN load) according to ISO standard 14577-1 (ISO 14577-1 2015). The Oliver and Pharr method (Oliver and Pharr 1992) was used to interpret the nanoindentation load-displacement graphs and an average of 50 indentations was reported as the hardness value. The depth where the indenter penetrated to the surface was on one hand 20 times higher than the surface roughness and on the other hand, below 10% of the coating thickness to minimize the uncertainty of hardness values. The

corrosion resistance of the substrates was tested by electrochemical potentiodynamic polarization method exposing a surface area of 1 cm² of substrates into open to air physiological saline solution (0.9% NaCl). All electrochemical potentiodynamic polarization measurements were carried out according to ASME standard G5 (ASTM G5 2015) at 298 K with a sweep rate of 0.6 V h⁻¹ on a GAMRY electrochemical analyzer (Warminster, USA). A three-electrode cell, using a saturated calomel as the reference electrode and graphite as the counter electrode, was set up for this purpose. The test started after about an hour immersing the specimen in the electrolyte to reach a steady state condition for the open circuit potential. Friction and wear tests were performed according to BS EN 1071-12 standard (BS EN1071-12 2010) using a wear test machine with ball-on-disk configuration (UTM with a 440-C martensitic steel ball, 10 N load). The test started after the samples were immersed in saline solution at room temperature.

**Fig. 1** a SEM cross-section, b surface micrograph, c surface roughness of chromium oxide coatings, and d surface roughness of bare 316L substrates

Ten thousand cycles with a displacement length of 2.5 mm was set in a linear reciprocating motion for all the samples. An inductively coupled plasma optical emission spectrometer (iCAP™ 7400 made by ThermoFisher Scientific, Massachusetts, USA) was employed to analyze the biocompatibility of the samples by probing the amount of toxic Cr ions released into the solution after 5 months immersion tests.

Results and discussion

Figure 1 a and b show the SEM images from cross-section and surface morphology of chromium oxide coatings, while Fig. 1 c and d compare the roughness of coatings and substrates, respectively. The coatings show dense nanocrystalline morphology with a very low roughness in the range of 1–2 nm. This smoothness of coatings can be an indication of coatings imitation from the bare substrate roughness during the film growth and nanocrystalline structure of coatings.

The structural analysis conducted by XRD (Fig. 2a) on chromium oxide coatings showed that the coatings were only composed of Cr_2O_3 phase as the peak positions were all matched with the corundum Cr_2O_3 peak positions according to (PDF-98-009-7850) databases. Raman spectroscopy was also employed to backup XRD data since it is a recognized technique to analyze both amorphous and crystalline oxide materials (Elton N. Kaufmann 2003). In Fig. 2b, Raman shifts observed at 305 cm^{-1} , 345 cm^{-1} , 547 cm^{-1} , and 606 cm^{-1} are well-matched with the Raman modes of crystalline Cr_2O_3 mentioned in literature (Brown et al. 1968; Shim et al. 2004; Kikuchi et al. 2005). Moreover, the existence of single Cr_2O_3 phase in the coatings was confirmed by the high-resolution Cr 2p XPS analysis. The Cr 2p high-resolution spectrum was composed of Cr $2p_{3/2}$ and Cr $2p_{1/2}$ splits with Cr $2p_{3/2}$ binding energy at 576.6 eV and the energy gap between the splits was 9.7 eV, which is consistent with Cr_2O_3 (Moulder et al. 1992). Therefore, both the Raman and XPS results agreed well with the XRD data and confirmed that coatings were only composed of stoichiometric Cr_2O_3 crystalline phases.

The adhesion quality of chromium oxide coatings was evaluated with Rockwell-C indentation tests, where the imprints were observed by an optical microscope for a sign of any failure or delamination. The results showed that the coatings conformed well to the indentation, indicating that they have an acceptable adhesion without any adhesive delamination (Fig. 3).

Figure 4 indicates the hardness and Young's modulus of bare 316L SS substrates and chromium oxide-coated substrates. The average hardness and Young's modulus values of chromium oxide-coated substrates are about 29.76 and 304.9 GPa, respectively, which is in agreement with the reported values for the bulk Cr_2O_3 in literature (Samsonov 1973; Kainarskii and Degtyareva 1977; Kao et al. 1989;

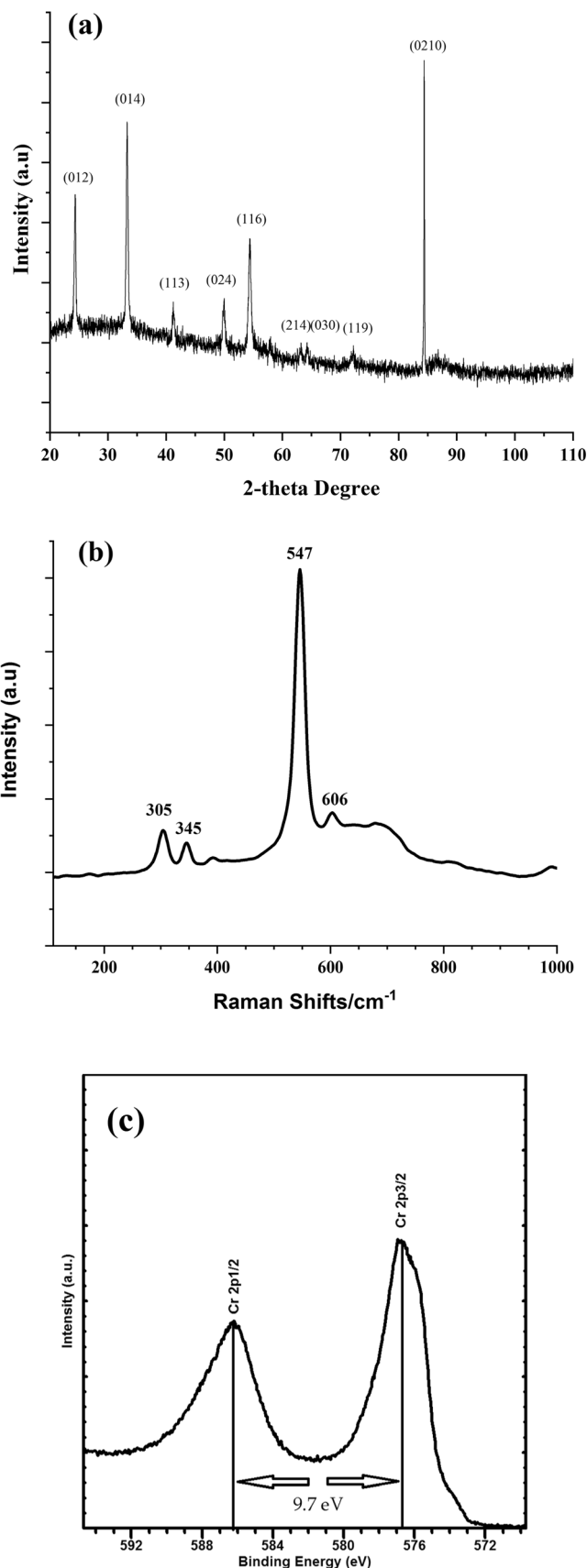


Fig. 2 a XRD patterns, b Raman spectra, and c the high-resolution Cr 2p XPS spectrum of deposited oxide coatings

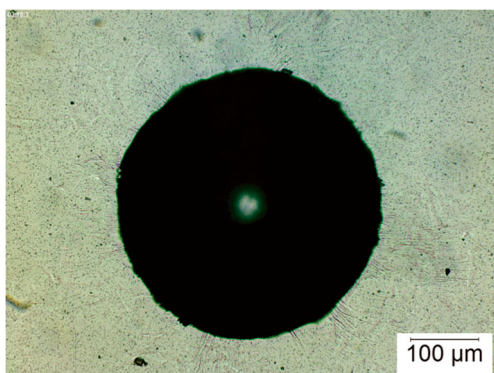


Fig. 3 Adhesion quality of chromium oxide coatings on SS316L substrates performed by Rockwell-C tester

Hones et al. 1999; Saeki et al. 2011). The bare 316L substrates have a hardness value significantly lower than chromium oxide coatings and in agreement with the literature reported values (Tromas et al. 2012).

Figure 5 shows the potentiodynamic polarization curves of the 316L SS and Cr_2O_3 -coated substrates obtained in a motionless open to air physiological saline solution at room temperature. Fitting the anodic and cathodic portion of polarization curves by a customized python module (Li et al. 2018) resulted in the Tafel plots and corrosion data. Table 2 compares the obtained corrosion data (corrosion potentials (E_{corr}), corrosion current densities (i_{corr}), and polarization resistance (R_p)) for both the 316L SS and Cr_2O_3 -coated substrates. Figure 5 shows that the samples obviously have a passivation region regardless of sample type and the corrosion resistance of the substrates is enhanced when they were coated by chromium oxide coatings.

Table 2 shows that the corrosion potential (E_{corr}) increases after applying chromium oxide coatings, with an E_{corr} of -0.41 V for bare 316L SS substrates and -0.19 V for the sample with the chromium oxide coatings. Furthermore, the corrosion rates can be evaluated by comparing the corrosion

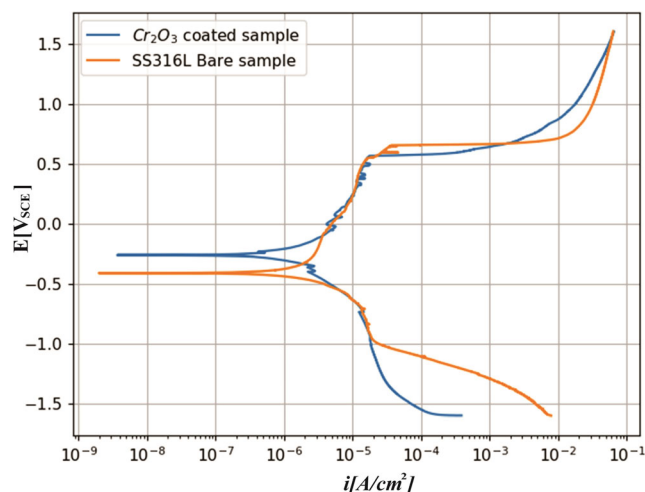


Fig. 5 Polarization curves for 316L stainless steel and Cr_2O_3 coated substrates

current densities. This is due to proportional relationship between the corrosion current densities and the kinetics of corrosion reactions. The corrosion current density of bare SS316L substrates is about $3 \mu\text{A}/\text{cm}^2$ which decreases to $1 \mu\text{A}/\text{cm}^2$ with applied chromium oxide coatings. The decrease in i_{corr} is a confirmation for the corrosion resistance improvement of Cr_2O_3 -coated samples when they are compared with the bare substrates. The R_p term is a definition for the charge transfer resistance in the solution–metal interface, which can be used as a parameter in anticipating the corrosion protection properties of coatings on metal surfaces (Liu et al. 2009). Based on the polarization resistance data, the chromium oxide coatings have improved the R_p from 30.662 to $40.156 \text{ K}\Omega$, so they can be an effective protective coating for 316L SS substrates in the physiological saline solutions.

Figure 6 shows the effect of chromium oxide coatings on the wear behavior and friction coefficient of bare SS316L substrates. After applying hard chromium oxide coatings, both

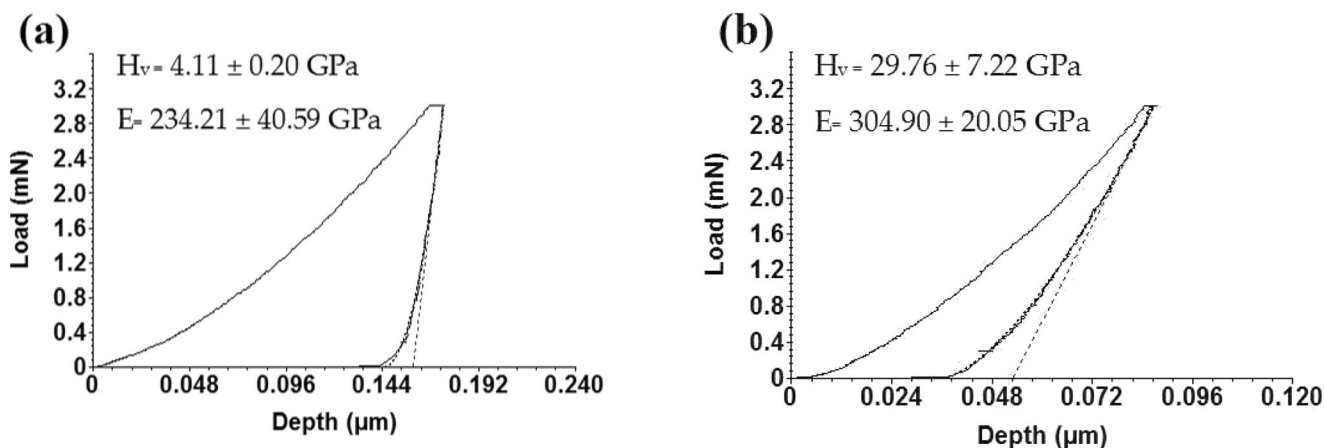


Fig. 4 **a** Indentation curve measured on bare SS316L and **b** indentation curve measured on a 1.5- μm -thick chromium oxide coating. H_v means the plastic Vickers hardness and E the elastic modulus corrected for deformation of the diamond

Table 2 Electrochemical parameters obtained from polarization curves in Fig. 5

Samples	E _{corr} (v)	I _{corr} (μA/cm ²)	R _p (KΩ)
Bare SS316L	-0.41	3	30.662
Cr ₂ O ₃ -Coated	-0.19	1	40.156

$$W = \frac{V}{2LSN}$$

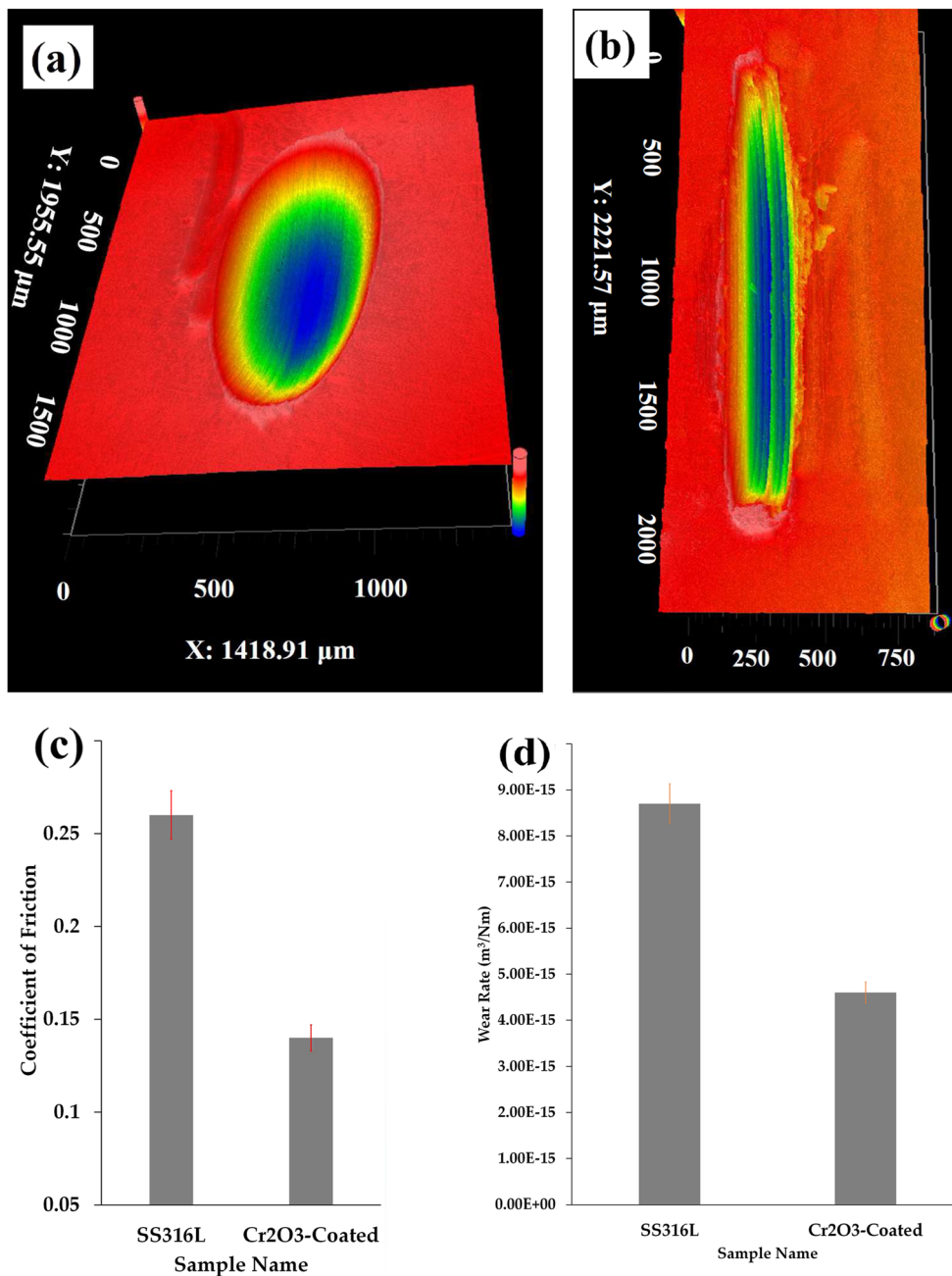
where *V* is the volume lost from substrates (m³); *L* is the applied load (N); *S* is the stroke length (m); *N* is the total number of reciprocations.

As shown in Fig. 6, the wear rate is about 50% lower for coated substrates compared to bare 316L SS. The friction coefficients, hardness, and film adhesion can influence the wear life of protective coatings (Da-Yung Wang 2001). Cr₂O₃ coatings act as solid lubricants and tend to reduce the friction coefficient (Jianjun et al. 1992). The

the wear rate and friction coefficient decreased significantly (Fig. 6c and d).

The wear rate of substrates can be calculated using the following formula (BS EN1071-12 2010):

Fig. 6 Tribological properties of bare and Cr₂O₃-coated SS316L substrates. **a** Wear volume of the bare substrate, **b** wear volume of the coated substrate, **c** coefficient of friction, and **d** wear rate of both bare and coated substrates



adhesion measurements (Fig. 3) confirm that chromium oxide coatings have good adhesion on SS316L substrates. Hence, the enhancement observed in the wear resistance can be attributed to the high hardness and low friction coefficient of chromium oxide coatings which also have good adhesion on 316L substrates.

Figure 7 illustrates the amount of toxic chromium ions released from substrates by probing saline solution used in the immersion tests. The optical emission spectroscopy results indicate that the chromium oxide-coated samples released negligible chromium ion about 0.01 ppm compared to 0.09 ppm for bare substrates.

Decreasing the chromium and nickel ions released from 316L steel in artificial body fluid media at 37 °C has been investigated by previous researchers; however, no significant success has been reported. In this regard, Diaz et al. (2008; Santonen et al. 2010) investigated the effect of passivation layer thickness on the amount of chromium and nickel ions released from 316L SS used as prosthetic implant materials in simulated body fluids. In their research, the passivation layer thickness was changed by an anodization process and the metal ion release was measured using atomic absorption spectroscopy after 1, 6, 11, and 15 days, respectively. They showed that the amount of nickel and chromium ions detected in body fluids were proportional to the passivation layer and increased from 2 to 10 times as the passivation layer increased. Moreover, two other researchers, Kocadereli et al.

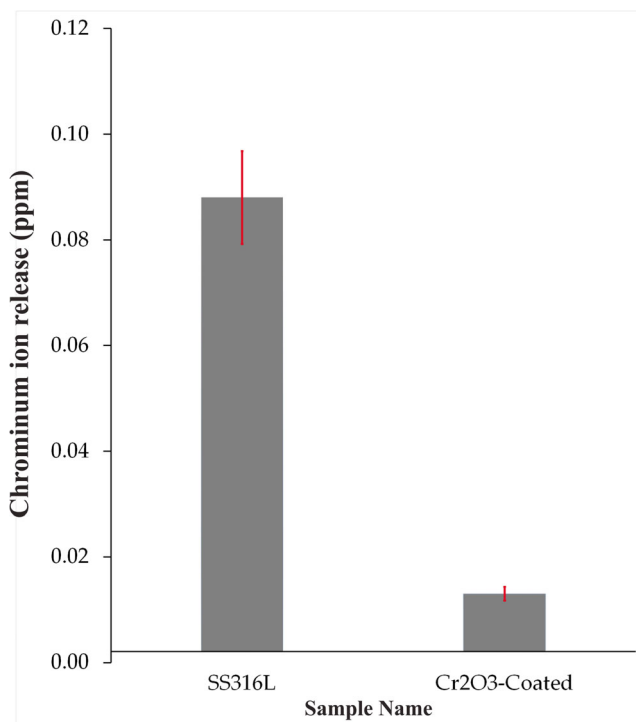


Fig. 7 Chromium ion released from substrates exposed to saline solution at 37 °C

(2000) and Ağaoğlu et al. (2001), investigated the amount of nickel and chromium ions released from SS orthodontic fixtures in the patients' salivary samples. They showed that considerable amounts of chromium and nickel are detected in the salivary samples. Therefore, our research implies that stoichiometric single-phase Cr₂O₃ coatings are a good candidate for enhancing the biocompatibility of SS implants in biological environments.

Conclusions

The compatibility of hard chromium oxide coatings prepared by reactive magnetron sputtering on SS316L substrates has been investigated for biomedical applications at room temperature in saline solution. According to structural and phase compositional analysis, dense stoichiometric single-phase Cr₂O₃ coatings were successfully prepared on the steel substrate at appropriate deposition parameters. The coatings have a high hardness and good adhesion on SS316L substrates. The corrosion results based on potentiodynamic polarization measurements showed an enhancement in corrosion resistance for chromium oxide-coated stainless steel samples compared to the bare SS substrate. The corrosion current density for chromium oxide-coated stainless steel is three times lower than uncoated stainless steel, suggesting the presence of a higher resistant passive film on the coatings. Tribological test results exhibited that Cr₂O₃ coated substrates possessed better wear resistance under sliding wear test conditions in saline solution. This can be related to the properties such as high hardness, low coefficient of friction, and good adhesion of chromium oxide coatings.

The ion release results from the ICP-OES measurements indicate that there were negligible chromium ions (at the parts per billion (ppb) level) released from the chromium oxide-coated samples into saline solution after 5 months immersion under testing conditions. These results indicated that hard Cr₂O₃ coatings can be a good candidate for extending the lifetime of biomedical stainless steel implants; however, more researches are required to pave the way for orthopedic and other possible medical implant applications of chromium oxide coatings.

Acknowledgments The authors would like to thank George Belev for performing XPS, Jianfeng Zhu for the grazing incidence XRD measurements, and Gang Li for interpretation of corrosion data.

Funding information This work was financially supported by the Natural Sciences and Engineering Research Council of Canada (NSERC), the Canada Foundation for Innovation (CFI), Western Economic Diversification Canada, and the University of Saskatchewan.

Compliance with ethical standards

Conflict of interest The authors declare that they have no conflict of interest.

References

- Ağaoğlu G, Arun T, Izgi B et al (2001) Nickel and chromium levels in the saliva and serum of patients with fixed orthodontic appliances. *Angle Orthod* 71:375–379. [https://doi.org/10.1043/0003-3219\(2001\)071<0375:NACLIT>2.0.CO;2](https://doi.org/10.1043/0003-3219(2001)071<0375:NACLIT>2.0.CO;2)
- Anttila A, Lappalainen R, Heinonen H, Santavirta SKY (1999) Superiority of diamond-like carbon coating on articulating surfaces of artificial hip joints. *New Diam Front Carbon Technol* 9:283–288
- ASTM G5 (2015) Standard reference test method for making potentiodynamic anodic polarization measurements. 1–9. <https://doi.org/10.1520/G0005-14.2>
- Babu PS, Sen D, Jyothirmayi A, Krishna LR, Rao DS (2018) Influence of microstructure on the wear and corrosion behavior of detonation sprayed $\text{Cr}_2\text{O}_3\text{-Al}_2\text{O}_3$ and plasma sprayed Cr_2O_3 coatings. *Ceram Int* 44:2351–2357. <https://doi.org/10.1016/j.ceramint.2017.10.203>
- Barshilia HC, Rajam KS (2008) Growth and characterization of chromium oxide coatings prepared by pulsed-direct current reactive unbalanced magnetron sputtering. *Appl Surf Sci* 255:2925–2931. <https://doi.org/10.1016/j.apsusc.2008.08.057>
- Bhushan B (1981) Structural and compositional characterization of Rf sputter-deposited Ni-Cr+ Cr_2O_3 films. *J Lubr Technol ASME* 103: 211–217
- Bhushan B, Theunissen GSAM, Li XD (1997) Tribological studies of chromium oxide films for magnetic recording applications. *Thin Solid Films* 311:67–80. [https://doi.org/10.1016/S0040-6090\(97\)00453-7](https://doi.org/10.1016/S0040-6090(97)00453-7)
- Brown DA, Cunningham D, Glass WK (1968) The infrared and Raman spectra of chromium (III) oxide. *Spectrochim Acta A Mol Spectrosc* 24:965–968. [https://doi.org/10.1016/0584-8539\(68\)80115-1](https://doi.org/10.1016/0584-8539(68)80115-1)
- BS EN1071-12 (2010) Advanced technical ceramics. Methods of test for ceramic coatings. Reciprocating wear test
- Carta G, Natali M, Rossetto G, Zanella P, Salmaso G, Restello S, Rigato V, Kaciulis S, Mezzi A (2005) A comparative study of Cr_2O_3 thin films obtained by MOCVD using three different precursors. *Chem Vap Depos* 11:375–380. <https://doi.org/10.1002/cvde.200406360>
- Charalambous CP (2014) Calcium phosphate ceramics as hard tissue prosthetics. In: *Classic papers in orthopaedics*. Springer London, London, pp 419–421
- Contoux G, Cosset F, Célérier A, Machet J (1997) Deposition process study of chromium oxide thin films obtained by d.c. magnetron sputtering. *Thin Solid Films* 292:75–84. [https://doi.org/10.1016/S0040-6090\(96\)08941-9](https://doi.org/10.1016/S0040-6090(96)08941-9)
- Da-Yung Wang M-CC (2001) Characterization of $\text{Cr}_2\text{O}_3/\text{CrN}$ duplex coatings for injection molding applications. *Surf Coat Technol* 137:164–169. <https://doi.org/10.1016/j.jmms.2003.12.245>
- Díaz M, Sevilla P, Galán AM, Escolar G, Engel E, Gil FJ (2008) Evaluation of ion release, cytotoxicity, and platelet adhesion of electrochemical anodized 316 L stainless steel cardiovascular stents. *J Biomed Mater Res Appl Biomater* 87B:555–561. <https://doi.org/10.1002/jbm.b.31144>
- Dong S, Song B, Hansz B, Liao H, Coddet C (2013) Microstructure and properties of Cr_2O_3 coating deposited by plasma spraying and dry-ice blasting. *Surf Coat Technol* 225:58–65. <https://doi.org/10.1016/j.surfcoat.2013.03.016>
- Kaufmann EN (2003) Raman spectroscopy of solids. In: *Characterization of materials*. John Wiley & Sons, Inc, pp 698–700
- Fisher J, Hu XQ, Stewart TD, Williams S, Tipper JL, Ingham E, Stone MH, Davies C, Hatto P, Bolton J, Riley M, Hardaker C, Isaac GH, BERRY G (2004) Wear of surface engineered metal-on-metal hip prostheses. *J Mater Sci Mater Med* 15:225–235. <https://doi.org/10.1023/B:JMSM.0000015482.24542.76>
- Fisher J, Hu XQ, Tipper JL, Stewart TD, Williams S, Stone MH, Davies C, Hatto P, Bolton J, Riley M, Hardaker C, Isaac GH, Berry G, Ingham E (2002) An in vitro study of the reduction in wear of metal-on-metal hip prostheses using surface-engineered femoral heads. *Proc Inst Mech Eng H J Eng Med* 216:219–230. <https://doi.org/10.1243/09544110260138709>
- Gotman I, Gutmanas EY (2014) Titanium nitride-based coatings on implantable medical devices. *Adv Biomater Devices Med* 1: 53–73
- Hones P, Diserens M, Lévy F (1999) Characterization of sputter-deposited chromium oxide thin films. *Surf Coatings Technol* 120–121:277–283. [https://doi.org/10.1016/S0257-8972\(99\)00384-9](https://doi.org/10.1016/S0257-8972(99)00384-9)
- ISO 14577-1 (2015) Metallic materials-instrumented indentation test for hardness and materials parameters-test method
- ISO 26443 (2002) Fine ceramics (advanced ceramics, advanced technical ceramics) — rockwell indentation test for evaluation of adhesion of ceramic coatings
- Ji AL, Wang W, Song G et al (2004) Microstructures and mechanical properties of chromium oxide films by arc ion plating. *Mater Lett* 58:1993–1998. <https://doi.org/10.1016/j.matlet.2003.12.029>
- Jianjun W, Xue Q, Wang H (1992) Friction and wear of Cr_2O_3 coating in inorganic salt solutions. *Wear* 152:161–170
- Kainarskii IS, Degtyareva EV (1977) Chromic oxide as refractory material. *Refractories* 18:42–47. <https://doi.org/10.1007/BF01319646>
- Kao AS, Doerner MF, Novotny VJ (1989) Processing effects on the tribological characteristics of reactively sputtered chromium oxide (Cr_2O_3) overcoat films. *J Appl Phys* 66:5315–5321. <https://doi.org/10.1063/1.343722>
- Kikuchi S, Kawauchi K, Kurosawa M et al (2005) Non-destructive rapid analysis discriminating between chromium(VI) and chromium(III) oxides in electrical and electronic equipment using Raman spectroscopy. *Anal Sci* 21:197–198. <https://doi.org/10.2116/analsci.21.197>
- Kocadereli L, Ataç PA, Kale PS, Ozer D (2000) Salivary nickel and chromium in patients with fixed orthodontic appliances. *Angle Orthod* 70:431–434. [https://doi.org/10.1043/0003-3219\(2000\)070<0431:SNACIP>2.0.CO;2](https://doi.org/10.1043/0003-3219(2000)070<0431:SNACIP>2.0.CO;2)
- Lackey WJ, Stinton DP, Cerny GA et al (1987) Ceramic coatings for advanced heat engines—A review and projection. *Adv Ceram Mater* 2:24–30. <https://doi.org/10.1111/j.1551-2916.1987.tb00048.x>
- Li G, Evitts R, Boulfiza M, Li ADS (2018) A customized Python module for interactive curve fitting on potentiodynamic scan data. <https://zenodo.org/record/1343975#.W6FZvc5KjIU>
- Lin J, Sproul WD (2015) Structure and properties of Cr_2O_3 coatings deposited using DCMS, PDCMS, and DOMS. *Surf Coat Technol* 276:70–76. <https://doi.org/10.1016/j.surfcoat.2015.06.044>
- Liu H, Tao J, Xu J, Chen Z, Gao Q (2009) Corrosion and tribological behaviors of chromium oxide coatings prepared by the glow-discharge plasma technique. *Surf Coat Technol* 204:28–36. <https://doi.org/10.1016/j.surfcoat.2009.06.020>
- Love CA, Cook RB, Harvey TJ, Dearnley PA, Wood RJK (2013) Diamond like carbon coatings for potential application in biological implants—a review. *Tribol Int* 63:141–150. <https://doi.org/10.1016/J.TRIBOINT.2012.09.006>
- Luo F, Gao K, Pang X, Yang H, Qiao L, Wang Y (2008) Characterization of the mechanical properties and failure

- modes of hard coatings deposited by RF magnetron sputtering. *Surf Coat Technol* 202:3354–3359. <https://doi.org/10.1016/j.surfcoat.2007.12.020>
- Luo F, Pang X, Gao K, Yang H, Wang Y (2007) Role of deposition parameters on microstructure and mechanical properties of chromium oxide coatings. *Surf Coat Technol* 202:58–62. <https://doi.org/10.1016/j.surfcoat.2007.04.066>
- Mohammadtaheri M, Yang Q, Li Y, Corona-Gomez J (2018) The effect of deposition parameters on the structure and mechanical properties of chromium oxide coatings deposited by reactive magnetron sputtering. *Coatings* 8:111. <https://doi.org/10.3390/coatings8030111>
- Monnereau O, Tortet L, Grigorescu CEA et al (2010) Chromium oxides mixtures in PLD films investigated by Raman spectroscopy. *J Optoelectron Adv Mater* 12:1752–1757
- Moulder JF, Stickle WF, Sobol PE, Bomben KD (1992) Handbook of X-ray photoelectron spectroscopy 261. <https://doi.org/10.1002/sia.740030412>
- Ningshen S, Kamachi Mudali U, Amarendra G, Gopalan P, Dayal RK, Khatak HS (2006) Hydrogen effects on the passive film formation and pitting susceptibility of nitrogen containing type 316L stainless steels. *Corros Sci* 48:1106–1121. <https://doi.org/10.1016/j.corsci.2005.05.003>
- Oje AM, Ogwu AA (2017) Chromium oxide coatings with the potential for eliminating the risk of chromium ion release in orthopaedic implants subject category. *R Soc open Sci* 4:170218. <https://doi.org/10.1098/rsos.170218>
- Oliver WC, Pharr GM (1992) An improved technique for determining hardness and elastic modulus using load and displacement sensing indentation experiments. *Mater Res Soc* 7:1564–1583
- Pang X, Gao K, Luo F, Yang H, Qiao L, Wang Y, Volinsky AA (2008) Annealing effects on microstructure and mechanical properties of chromium oxide coatings. *Thin Solid Films* 516:4685–4689. <https://doi.org/10.1016/j.tsf.2007.08.083>
- Roy RK, Lee K-R (2007) Biomedical applications of diamond-like carbon coatings: a review. *J Biomed Mater Res B Appl Biomater* 83B:72–84. <https://doi.org/10.1002/jbm.b.30768>
- Saeki I, Ohno T, Seto D, Sakai O, Sugiyama Y, Sato T, Yamauchi A, Kurokawa K, Takeda M, Onishi T (2011) Measurement of Young's modulus of oxides at high temperature related to the oxidation study. *Mater High Temp* 28:264–268. <https://doi.org/10.3184/096034011X13182685579795>
- Samsonov GV (1973) *The oxide handbook*. IFI/Plenum press
- Santonen T, Stockmann H, ZITTING A (2010) Review on toxicity of stainless steel
- Serro AP, Completo C, Colaço R, dos Santos F, da Silva CL, Cabral JMS, Araújo H, Pires E, Saramago B (2009) A comparative study of titanium nitrides, TiN, TiNbN and TiCN, as coatings for biomedical applications. *Surf Coat Technol* 203:3701–3707. <https://doi.org/10.1016/J.SURFCOAT.2009.06.010>
- Shim S-H, Duffy TS, Jeanloz R, Yoo CS, Iota V (2004) Raman spectroscopy and x-ray diffraction of phase transitions in Cr₂O₃ to 61 GPa. *Phys Rev B* 69:144107. <https://doi.org/10.1103/PhysRevB.69.144107>
- Singh VP, Sil A, Jayaganthan R (2012) Wear of plasma sprayed conventional and nanostructured Al₂O₃ and Cr₂O₃, based coatings. *Trans Indian Inst Metals* 65:1–12. <https://doi.org/10.1007/s12666-011-0070-0>
- Sourty E, Sullivan JL, Bijker MD (2003) Chromium oxide coatings applied to magnetic tape heads for improved wear resistance. *Tribol Int* 36:389–396. [https://doi.org/10.1016/S0301-679X\(02\)00214-1](https://doi.org/10.1016/S0301-679X(02)00214-1)
- Sousa PM, Silvestre AJ, Conde O (2011) Cr₂O₃ thin films grown at room temperature by low pressure laser chemical vapour deposition. *Thin Solid Films* 519:3653–3657. <https://doi.org/10.1016/J.TSF.2011.01.382>
- Taeger G, Podleska LE, Schmidt B, Ziegler M, Nast-Kolb D (2003) Comparison of diamond-like-carbon and alumina-oxide articulating with polyethylene in total hip arthroplasty. *Materwiss Werksttech* 34:1094–1100. <https://doi.org/10.1002/mawe.200300717>
- Tromas C, Stinville JC, Templier C, Villechaise P (2012) Hardness and elastic modulus gradients in plasma-nitrided 316L polycrystalline stainless steel investigated by nanoindentation tomography. *Acta Mater* 60:1965–1973. <https://doi.org/10.1016/J.ACTAMAT.2011.12.012>
- Trube J (1993) Low stress and optically transparent chromium oxide layer for x-ray mask making. *J Vac Sci Technol B Microelectron Nanom Struct* 11:2990. <https://doi.org/10.1116/1.586574>
- van Hove RP, Sierevelt IN, van Royen BJ, Nolte PA (2015) Titanium-nitride coating of orthopaedic implants: a review of the literature. *Biomed Res Int* 2015:1–9. <https://doi.org/10.1155/2015/485975>

Publisher's note Springer Nature remains neutral with regard to jurisdictional claims in published maps and institutional affiliations.